Tidal front around the Hainan Island, northwest of the South China Sea

Jianyu Y. Hu,[1] Hiroshi Kawamura, and Danling L. Tang[2]

Center for Atmospheric and Oceanic Studies, Institute of Hydrobiology, Faculty of Science, Tohoku University, Sendai, Japan

Received 3 April 2003; revised 20 June 2003; accepted 10 September 2003; published 6 November 2003.

[1] As the coastal fronts being detected by the SeaWiFS-derived Chl-a concentrations and AVHRR-derived SST images, a three-dimensional primitive equation numerical model is used to study the physical mechanisms for the formation of fronts around the Hainan Island, northwest of the South China Sea. Several monthly averaged SeaWiFS-derived Chl-a concentrations indicate that higher Chl-a zones usually exist along the coasts of the Zhanjiang Peninsula, the Beibu Gulf (or the Gulf of Tonkin) and the Hainan Island. Obvious surface Chl-a fronts can thus be seen narrowly adjacent to the higher Chl-a zones. AVHRR-derived SST images indicate several other fronts that have a large seasonal variation. The SST fronts are formed in the Beibu Gulf and in the northeastern area off the Hainan Island in winter. The numerical modeling of seven major tidal constituents (M_2, S_2, K_1, O_1, P_1, N_2, and K_2) indicates that two high kinetic energy zones appear in the Qiongzhou Strait and near the southwestern coast of the Hainan Island. The value of log (h/u^3), where h is depth in meter and u is the depth-mean tidal current in m/s, is calculated to predict the frontal position. It is indicated that the locations of contour lines log (h/u^3) = 2.9 $\sim$ 3.0 are in good agreement with the frontal positions detected by the satellite observations. Therefore these Chl-a fronts can be considered to be mainly induced by the tidal mixing while the monsoon wind, solar radiation, and coastal dynamics may play an important role for the seasonal variation of several other fronts. *INDEX TERMS:* 4528 Oceanography: Physical: Fronts and jets; 4255 Oceanography: General: Numerical modeling; 4275 Oceanography: General: Remote sensing and electromagnetic processes (0689); 4223 Oceanography: General: Descriptive and regional oceanography; *KEYWORDS:* tidal front, Beibu Gulf (Gulf of Tonkin), satellite observations, numerical modeling

Citation: Hu, J. Y., H. Kawamura, and D. L. Tang, Tidal front around the Hainan Island, northwest of the South China Sea, *J. Geophys. Res.*, *108*(C11), 3342, doi:10.1029/2003JC001883, 2003.

1. Introduction

[2] The Hainan Island is a big island located in the northwest of the South China Sea. The depth is about 20 $\sim$ 80 m around the Hainan Island. Depth contours shown in Figure 1a tongues from the South China Sea to the head of the Beibu Gulf (or the Gulf of Tonkin by some other references) through the sea area south of the Hainan Island. To the north of the Hainan Island, a narrow strait, called the Qiongzhou Strait, separates the island from the Zhanjiang Peninsula. To the west is the Beibu Gulf, which has the depth less than 80 m. The southeastern sea area is a narrow continental shelf followed by a steep continental slope. Obviously, the bottom topography around the Hainan Island is complex, which may have a great influence on the hydrography there.

[3] The tides around the Hainan Island have usually been mentioned in the researches on the tides in the South China Sea or the Beibu Gulf [e.g., *Ye and Robinson*, 1983; *Yu*, 1984; *Fang*, 1986; *Cao and Fang*, 1990; *Huang et al.*, 1994; *Yanagi et al.*, 1997; *Liu and Zhang*, 1997; *Manh and Yanagi*, 1997, 2000; *Fang et al.*, 1999; *Hu et al.*, 2001; *Li et al.*, 2001; *Sun and Huang*, 2001; *Shi et al.*, 2002]. A successful numerical modeling of four principal tidal constituents (M_2, S_2, K_1 and O_1) by *Fang et al.* [1999] indicated that the tidal waves usually propagate toward the Beibu Gulf from the south of the Hainan Island. In the Beibu Gulf, the co-tidal lines of M_2 tidal constituent appear as a degenerate amphidrome with smallest amplitude near the Red River in the northwestern head of the gulf. The overall magnitude of M_2 tide in the Beibu Gulf is significantly smaller than that of both K_1 and O_1. These characteristics have also been confirmed by *Hu et al.* [2001] who derived eight principal tidal constituents (M_2, S_2, K_1, O_1, P_1, Sa, N_2, and K_2) from 6 years of TOPEX/Poseidon altimeter data.

[4] Temperature front or tidal front has frequently been observed near the continental shelf in the world oceans

[1] Now at Marine Environmental Laboratory of Ministry of Education, Institute of Subtropical Oceanography, Xiamen University, Fujian, China.

[2] Also at Institute of Hydrobiology, Jinan University, Guangzhou, China.

0148-0227/03/2003JC001883$09.00

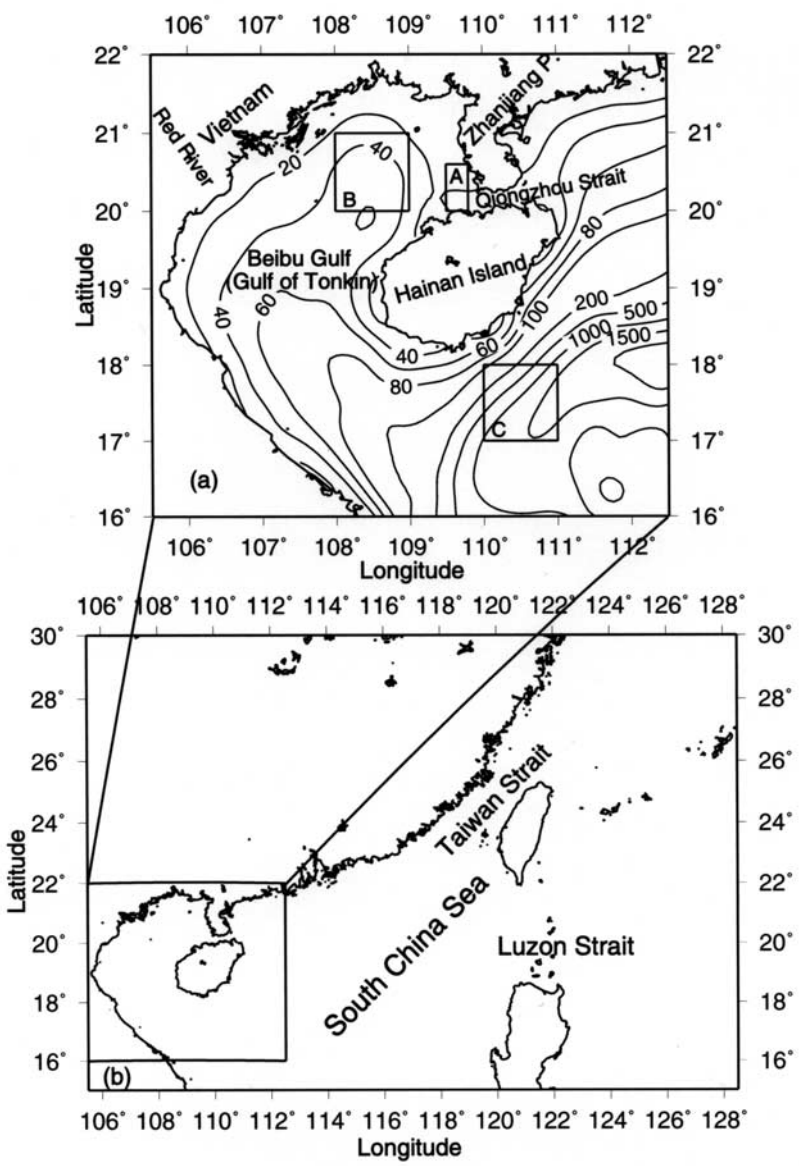

Figure 1. Map of the northern South China Sea and its adjacent areas. (a) Map of the studied area around the Hainan Island, with the depth contour in meters. (b) Computational domain of the tidal numerical model.

[e.g., *Simpson and Hunter*, 1974; *Pingree and Griffiths*, 1978; *Simpson et al.*, 1978; *Simpson*, 1981; *Simpson and Bowers*, 1979, 1981; *Hsueh and Cushman-Roisin*, 1983; *Bowers and Simpson*, 1987; *Yanagi and Koike*, 1987; *Stigebrandt*, 1988; *Lie*, 1989; *Yanagi and Tamaru*, 1990; *Yanagi et al.*, 1995; *Qi and Su*, 1998; *Xing and Davies*, 2001; *Chu and Wang*, 2003]. Moreover, two special issues on ocean fronts have been newly published in *Journal of Marine Systems* [*Belkin*, 2002] and *Dynamics of Atmospheres and Oceans* [*Belkin and Spall*, 2002], suggesting that the fronts have attracted many oceanographers' attention.

[5] Recently, the fronts in the northern South China Sea have been detected by satellite data. *Wang et al.* [2001, 2002] described the thermal fronts in the Beibu Gulf using 8 years of the Pathfinder sea surface temperature (SST) satellite data. It is indicated that the thermal fronts are the strongest in spring. Then the fronts reduce their coverage areas as well as their strength in summer and in winter. There are very few fronts in autumn. *Tang et al.* [2003] studied the chlorophyll-a (Chl-a) distributions in the Beibu Gulf using SeaWiFS-derived Chl-a data, indicating several Chl-a fronts in the Beibu Gulf. A previous study also showed fronts accompanied by the high pigment concentration areas in the Qiongzhou Strait and along the western coast of the Hainan Island, by analyzing annual CZCS images obtained during 1979 and 1986 [*Tang et al.*, 1998]. However, the physical mechanisms for the fronts in the northern South China Sea or around the Hainan Island are still lacking.

[6] A three-dimensional primitive equation numerical model is used to study the physical mechanisms for the formation of fronts around the Hainan Island. Section 2 presents the fronts detected by the satellite observations. In

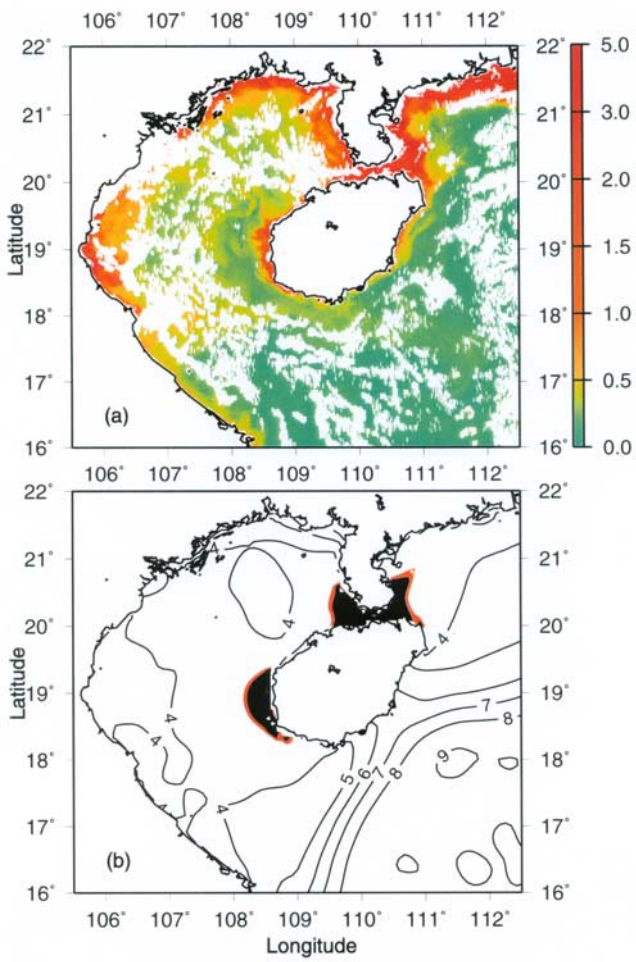

Figure 2. (a) Snapshot cloud-free SeaWiFS-derived Chl-a image on August 19 of 1999 and (b) log (h/u^3) contour lines in the studied area around the Hainan Island. The unit of Chl-a concentration is in mg m^{-3} in Figure 2a, and the areas with the value of log (h/u^3) less than 2.9 are shaded in black color while the contour lines with the value of log (h/u^3) = 2.9 $\sim$ 3.0 are marked in red in Figure 2b.

section 3, the numerical model is briefly mentioned and examined. Sections 4 and 5 describe the results of numerical experiments and discuss about the fronts around the Hainan Island, respectively. Section 6 is a summary of this study.

2. Front Detected by Satellite Observations

[7] Several fronts have been captured by satellite images in recent years. Figure 2a presents a cloud-free snapshot image of the SeaWiFS-derived Chl-a concentrations on August 19 of 1999 (see *Tang et al.* [2003] for data processing and verification). It is indicated that high Chl-a zones exist along the coasts of the Zhanjiang Peninsula and the Beibu Gulf, in the Qiongzhou Strait and near the southwestern coast of the Hainan Island. Evidently, surface Chl-a fronts are formed narrowly adjacent to these high Chl-a zones.

[8] The monthly averaged SeaWiFS-derived Chl-a concentrations also provide evidences for the existing Chl-a fronts. It is shown from Figure 3 that high Chl-a zones are distributed along the coasts of the Zhanjiang Peninsula and the Beibu Gulf and in the Qiongzhou Strait. The higher Chl-a concentration (>1 mg m^{-3}) appears in the Qiongzhou Strait. The low Chl-a concentration water extends toward the central Beibu Gulf through the southern sea area off the Hainan Island. From Figure 3, the Chl-a concentrations in summer (Figure 3a for the Chl-a distributions in August 2000) are lower than those in winter (Figure 3b for December 2000).

[9] In summer, a low Chl-a (less than 0.1 mg m^{-3}) area exists in the southeastern sea area off the Hainan Island, but the Chl-a is a little higher near the coast. Along the western and northern coasts of the Beibu Gulf, where the depth is shallower than 20 m, a strong front is formed with the high Chl-a greater than 1 mg m^{-3}. Two other strong fronts are seen at both ends of the Qiongzhou Strait and along the eastern coast of the Zhanjiang Peninsula.

[10] In winter, the southeastern sea area of the Hainan Island is also characterized with low Chl-a (about 0.3 mg m^{-3}). The fronts along the coasts of the Beibu Gulf, the Zhanjiang Peninsula and in the Qiongzhou Strait are almost the same as those in summer, but the Chl-a concentrations are higher; especially the central part of the Beibu Gulf also has relatively higher Chl-a concentrations. As for spring and autumn, those fronts also exist (see Figures 3c and 3d for April and October 2000, respectively).

[11] In order to investigate the seasonal variability of Chl-a concentrations in the frontal water (20.0°N–20.6°N, 109.5°E–109.8°E, denoted by box A in Figure 1a), the Beibu Gulf water (20°N–21°N, 108°E–109°E, box B), and the non-frontal water (17°N–18°N, 110°E–111°E, box C), the monthly averaged Chl-a values in these areas are calculated for September 1997 to March 2003 using the SeaWiFS-derived Chl-a concentrations. Figure 4 shows seasonal variations of the Chl-a concentrations in these areas. In the non-frontal water, the Chl-a concentrations are low because of limited nutrients and the amplitude of seasonal variation is quite small. In the Beibu Gulf water, the Chl-a concentrations have a seasonal peak in winter because of nutrient uptake caused by the strong monsoonal wind [*Tang et al.*, 2003]. In the frontal water, the Chl-a concentrations are high for all seasons, especially in winter. Even in summer, the frontal water maintains a level of Chl-a concentration much higher than those of the Beibu Gulf water and the non-frontal water. This may be attributed to the effects of tidal mixing examined in the present paper.

[12] AVHRR-derived SST images [*Tang et al.*, 2003] depict several other SST fronts. As shown in Figure 5, the monthly averaged SST distributions have a large seasonal variation. It has high SST greater than 28°C for the entire area around the Hainan Island, so no obvious front can be seen around the Hainan Island in summer (Figure 5a for the SST distribution in August 2000), but it shows large SST gradient with the SST fronts being formed in winter (Figure 5b for December 2000). As shown in Figure 5b, the front is located near the 80 m depth contour in the eastern coast of the Hainan Island, where the SST changes from 21°C to 23°C in a narrow belt of about 10 km in width, so the strength of the SST front reaches 0.2°C/km. In the Beibu Gulf, the warm water tongues toward the central part of the gulf from the southern sea area of the Hainan Island, and then forms a front when meeting with the cold water along

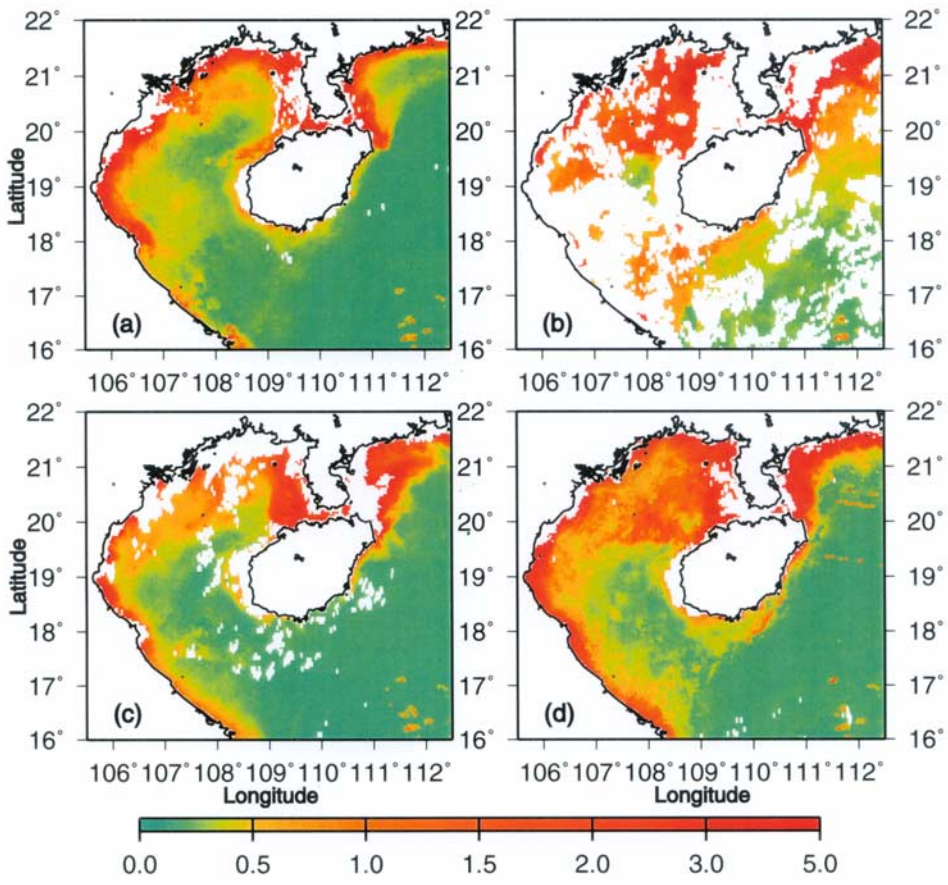

Figure 3. Monthly mean SeaWiFS-derived Chl-a images. (a) August 2000, (b) December 2000, (c) April 2000, and (d) October 2000. The unit of Chl-a concentration is in mg m^{-3}.

the northern and western coasts of the Beibu Gulf. The wintertime SST front pattern in the Beibu Gulf agrees well with that illustrated in the horizontal and vertical distributions of observed temperature, salinity and sigma-t [*Manh and Yanagi*, 2000]. Spring and autumn are transitional seasons for the monsoon in the South China Sea, so the SST patterns in spring and in autumn (Figure 5c for April 2000 and Figure 5d for November 2000) are close to those in summer and in winter, respectively.

3. Numerical Model

3.1. Model Description

[13] In order to explain the generating mechanism for the fronts around the Hainan Island, Princeton Ocean Model (POM [*Blumberg and Mellor*, 1987]) is used to simulate the major tidal constituents in the studied area.

[14] POM is a sigma coordinate model in that the vertical coordinate is scaled on the water column depth. In the present study, the depth is divided as seven layers vertically (0.000, −0.167, −0.333, −0.500, −0.667, −0.833, −1.000). The model has a horizontal grid spacing of 1/12° in longitude × 1/12° in latitude (about 9.26 km) and is applied to a larger computational domain between 105.5°E–128.5°E and 15.0°N–30.0°N (see Figure 1b). The temperature and salinity are set as constant values of 27°C and 34, respectively. There are no wind stress, heat and river discharge being inputted into the model because this study is mainly focused on the tidal mixing and its influence on generating the fronts in the studied area around the Hainan Island (Figure 1a). The governing equations used in the present study are the same as those appearing in the POM users guide [*Mellor*, 1998].

[15] For the larger computational domain shown in Figure 1b, there are three open boundaries, located in the south, east, and north, respectively. Since this area is dominated by seven principal tidal constituents [*Hu et al.*, 2001], that is, M_2, S_2, K_1, O_1, P_1, N_2 and K_2, these principal tidal constituents are selected accordingly.

[16] These tidal constituents are set at the same time along three open boundaries. That is,

$$\zeta = \sum f_c H_c \cos\left[\omega_c t + (V_0 + u)_c - g_c\right],$$

where H_c and g_c are the altimeter-derived harmonic constants for amplitude and phase, respectively. The angular speed of the tidal constituent is ω_c; and f_c and u_c represent nodal factor and nodal angle, respectively. V_{0c} is the initial phase angle of the equilibrium tide. The subscripted c denotes each tidal constituent. The parameters f_c, u_c, and V_{0c} are calculated by using several astronomical constants [*Fang et al.*, 1986].

[17] The harmonic constants of each considered tidal constituent at the open boundaries are derived from 6 years of TOPEX/Poseidon altimeter data [*Hu et al.*, 2001]. After

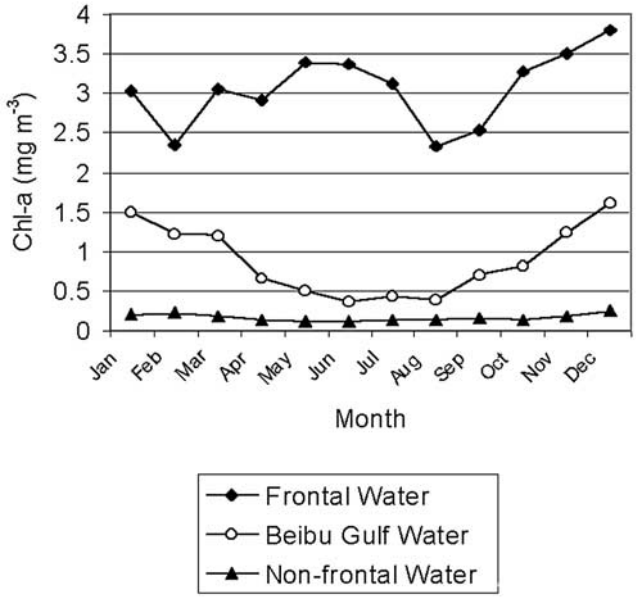

Figure 4. Seasonal variations of the Chl-a concentrations in the frontal water (20.0°N–20.6°N, 109.5°E–109.8°E, denoted by box A in Figure 1a), the Beibu Gulf water (20°N–21°N, 108°E–109°E, box B) and the non-frontal water (17°N–18°N, 110°E–111°E, box C). Time series of the monthly averaged SeaWiFS-derived Chl-a concentrations in these areas are calculated from September 1997 to March 2003, and then the seasonal variations are obtained.

interpolating the altimeter-derived harmonic constants to the grid points along the open boundaries, a reliable open boundary condition is constructed.

[18] The simulation begins from a state of rest using the external time step of 15 s. In the simulation, the realistic bottom topography and coastal lines are used. The depth data are taken from the ETOPO5 depth data set.

3.2. Model Test

[19] Before conducting the numerical experiments using multiple constituents, single tidal constituent computation is run for tests, which indicate that the sea surface elevation and velocity have a stable periodic oscillation after a simulation time of no more than 10 days. Both sea surface elevation and depth-mean velocities show very small differences respectively at each inside grid point for the successive tidal period. This means that the POM model is suitable to be applied to investigate tidal phenomena in the studied area.

[20] For the simulation forced by seven tidal constituents at three open boundaries, 375 days of tidal computations are conducted and the daily outputs of sea surface elevation and depth-mean velocities at all inside grids for 1 year beginning from the eleventh computing day have been reanalyzed using the harmonic method presented by *Fang et al.* [1986]. The simulated results indicate that the co-tidal charts of all these principal tidal constituents are in good agreement with those derived from satellite altimeter data [*Yanagi et al.*, 1997; *Hu et al.*, 2001], numerical results [*Fang et al.*, 1999], and in situ observational results [*Fang*, 1986; *Huang et al.*, 1994].

[21] As specified for the co-tidal charts around the Hainan Island, *Liu and Zhang* [1997], *Manh and Yanagi* [1997], and *Sun and Huang* [2001] developed the local tidal models (three-dimensional or two-dimensional numerical model) to simulate some major tidal constituents in the Beibu Gulf. For example, *Liu and Zhang* [1997] simulated six tidal constituents (M_2, S_2, N_2, K_1, O_1, and P_1) together. The simulated results agreed very well with observed ones at several tidal stations both in the Beibu Gulf and along the coast. When our simulated results are compared with these

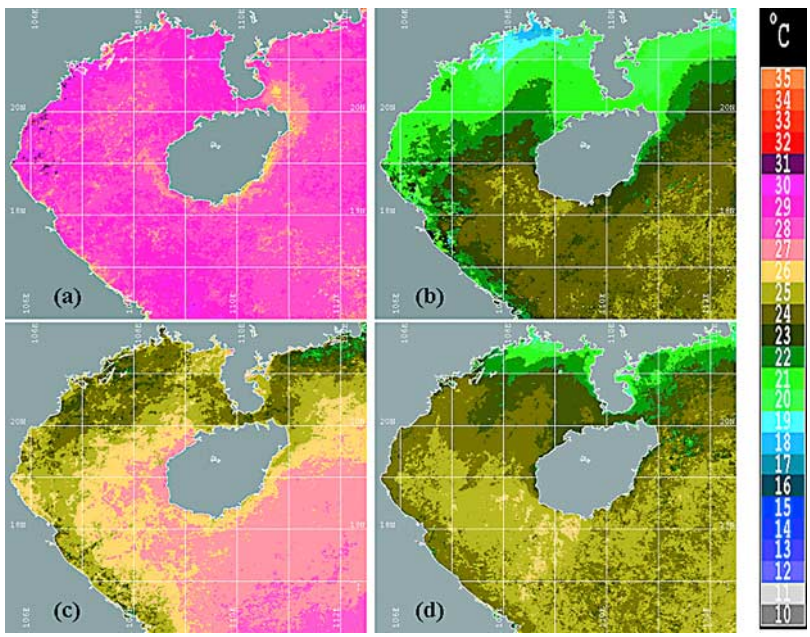

Figure 5. Monthly mean AVHRR-derived SST images. (a) August 2000, (b) December 2000, (c) April 2000, and (d) November 2000.

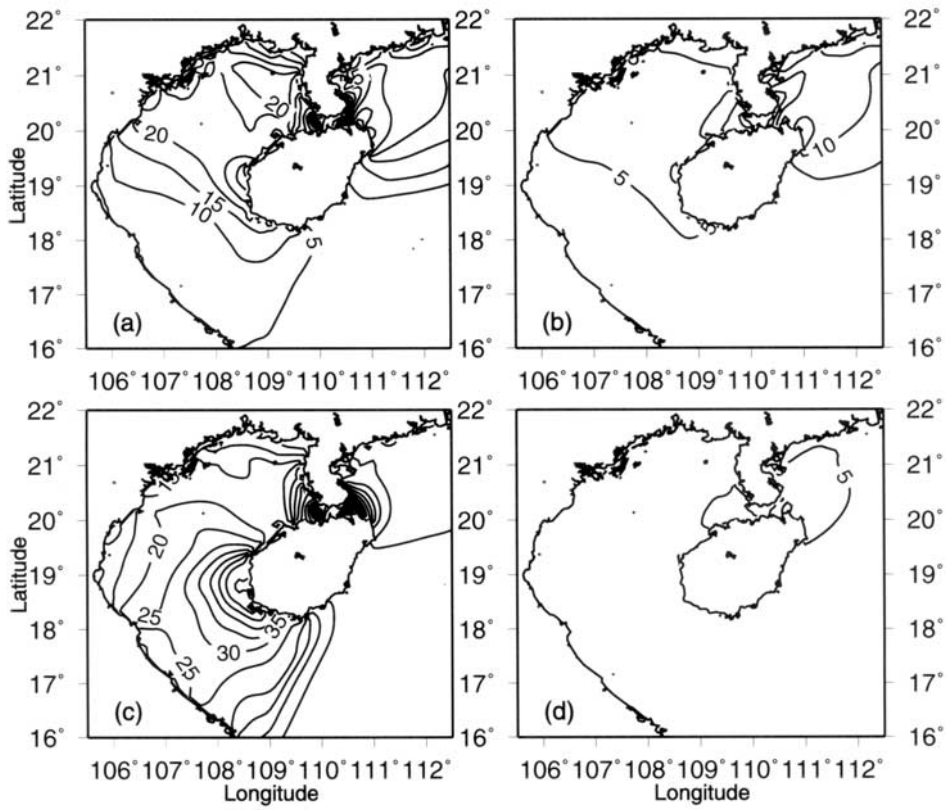

Figure 6. Maximum tidal current contours for four tidal constituents. (a) M_2 tidal constituent, (b) S_2 tidal constituent, (c) K_1 tidal constituent, and (d) K_2 tidal constituent. The unit of tidal current is in cm/s.

local model results, the co-tidal charts are almost the same for the Beibu Gulf and around the Hainan Island.

4. Numerical Model Results

[22] In order to quantify the contribution for tidal mixing made by respective tidal constituent, Figure 6 illustrates the maximum tidal current contours of four tidal constituents around the Hainan Island, which are consistent with some previous results such as *Manh and Yanagi* [1997] and *Sun and Huang* [2001]. After the tidal simulation for the larger computational domain, the results in the studied area around the Hainan Island are sampled for further examination. It is indicated that the strong tidal currents are located in the Qiongzhou Strait and near the southwestern coast of the Hainan Island, but the location and strength are different for respective tidal constituent. For the M_2 tidal constituent, the strongest tidal currents appear in the Qiongzhou Strait with the maximum speed of more than 70 cm/s, but there only exists a small area of strong tidal current (more than 25 cm/s in speed) near the southwestern coast of the Hainan Island (Figure 6a). The maximum tidal currents of the S_2 tidal constituent are weaker than those of the M_2 tidal constituent, they are about 20 cm/s in the Qiongzhou Strait (Figure 6b). The K_1 tidal constituent, as well as the O_1 tidal constituent, is dominant and has a similar distribution pattern of the maximum tidal current around the Hainan Island. Both of them exceed 80 cm/s in the Qiongzhou Strait and exceed 50 cm/s near the southwestern coast of the Hainan Island. The strong tidal currents cover a larger area in the southwest of the Hainan Island (see Figure 6c for the K_1 tidal constituent). As for the other three tidal constituents (P_1, N_2, and K_2), the tidal currents are not so strong. The maximum tidal currents are only 5 cm/s for K_2 (see Figure 6d), about $5 \sim 10$ cm/s for N_2 and about $20 \sim 30$ cm/s for P_1.

[23] Figure 7 depicts the mean kinetic energy of the total seven tidal constituents in the studied area. It is indicated that a high kinetic energy zone appears in the Qiongzhou Strait where the kinetic energy is greater than 15×10^{-2} m^2/s^2. In the southwestern coastal area of the Hainan Island, another high kinetic energy zone appears with the higher energy nearshore (greater than 8×10^{-2} m^2/s^2). The southeastern sea area of the Hainan Island and the continental coastal areas of the Beibu Gulf are characterized with low kinetic energy of about $1 \sim 2 \times 10^{-2}$ m^2/s^2.

[24] *Simpson and Hunter* [1974] first proposed the parameter of log (h/u^3) to indicate the frontal position. We also calculate the value of log (h/u^3), where h is depth in meter and u is the depth-mean tidal current in m/s. Here u is calculated from a time average of tidal currents over 1 year as mentioned by *Loder and Greenberg* [1986]. It is obvious from Figure 2b that the log (h/u^3) contour lines with the value less than 3.0 exist in the Qiongzhou Strait and near the southwestern coast of the Hainan Island (see the marked areas in Figure 2b). The contour lines with smaller log (h/u^3) value can also extend to both eastern and western coasts of the Zhanjiang Peninsula. These areas are regarded as well-mixed areas because of the strong tidal currents. The

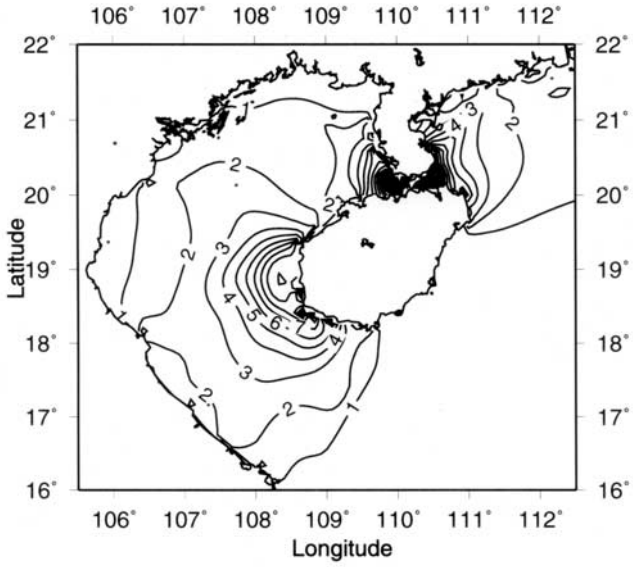

Figure 7. Mean kinetic energy in the studied area around the Hainan Island. The unit of the kinetic energy is in 10^{-2} m^2/s^2.

locations of contour lines log (h/u^3) = 2.9 ~ 3.0, marked in red color in Figure 2b, show almost the same patterns as the surface Chl-a front detected by the SeaWiFS and can thus be considered as the tidal frontal positions [e.g., *Simpson and Hunter*, 1974; *Bowers and Simpson*, 1987; *Lie*, 1989; *Yanagi et al.*, 1995].

[25] Figure 8 illustrates the contours of log (h/u^3) for four respective tidal constituent, indicating that the contribution for tidal mixing made by respective tidal constituent is quite different. Here u is the amplitude of depth-mean tidal current calculated from the tidal current harmonic constants of each tidal constituent. For the M_2 tidal constituent, the log (h/u^3) contour lines with the value less than 3.0 exist in the Qiongzhou Strait and a small nearshore area southwest of the Hainan Island (see the shaded areas in Figure 8a). However, there is no area with the value of log (h/u^3) less than 3.0 for the S_2 tidal constituent (Figure 8b). Figure 8c shows that both the Qiongzhou Strait and the southwestern coastal area of the Hainan Island have the log (h/u^3) contour lines with the value less than 3.0 for the K_1 tidal constituent. And O_1 tidal constituent has almost the similar log (h/u^3) contour lines as the K_1 tidal constituent does. For the other three tidal constituents (P_1, N_2, and K_2), the values of log (h/u^3) are relatively larger in the studied area; therefore, there is no area with the value of log (h/u^3) less than 3.0 for the N_2 and K_2 tidal constituents (see Figure 8d for the K_2 tidal constituent) but only a very small area in the central Qiongzhou Strait for the P_1 tidal constituent. It can be regarded that the M_2, K_1, and O_1 tidal constituents play important roles on tidal mixing in the Qiongzhou Strait while the K_1 and O_1 tidal constituents act for tidal mixing in the southwestern coastal area of the Hainan Island. The S_2, P_1, N_2, and K_2 tidal constituents play less of a role in tidal

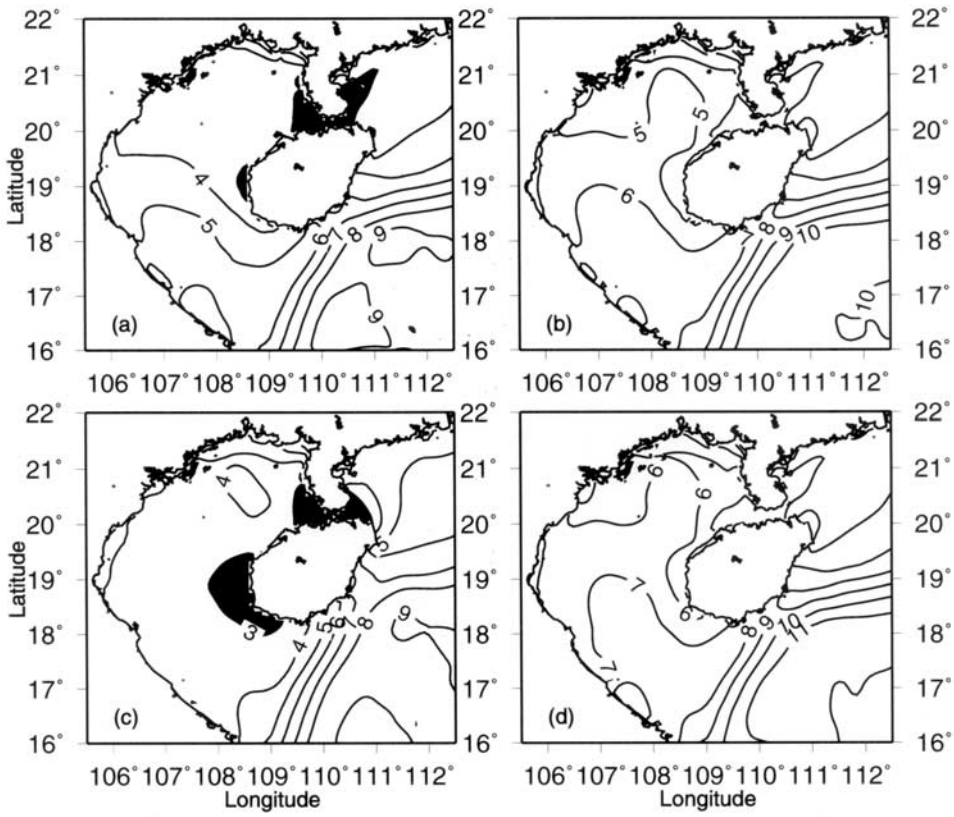

Figure 8. The log (h/u^3) contour lines for four tidal constituents. (a) M_2 tidal constituent, (b) S_2 tidal constituent, (c) K_1 tidal constituent, and (d) K_2 tidal constituent. The areas with the value of log (h/u^3) less than 3.0 are shaded.

mixing in the studied area; especially the N_2 and K_2 tidal constituents can be negligible due to their weak tidal currents.

5. Discussions

[26] The numerical model of tides predicts the occurrence of the log (h/u^3) criterion with several Chl-a fronts detected by the satellite observations. The tidal currents are quite strong in the Qiongzhou Strait and along the eastern and western coasts of the Zhanjiang Peninsula. The strong tidal currents stir up the nutrient-rich water from the lower layers and make these areas have higher Chl-a concentrations. The fronts are thus formed narrowly adjacent to these higher Chl-a areas. Therefore, tidal mixing is considered as a main cause for inducing these surface Chl-a fronts in these areas.

[27] From the tidal numerical model result, another well-mixed area is located in the southwestern sea area off the Hainan Island. However, the monthly averaged Chl-a distributions (see Figure 3) do not demonstrate corresponding high Chl-a concentrations in this area. The Chl-a data are usually masked by the present SeaWiFS Chl-a algorithm. From the snapshot cloud-free SeaWiFS Chl-a image as shown in Figure 2a, it is obvious that there exists a high Chl-a area near the southwestern coast of the Hainan Island, almost the same area as the well-mixed area revealed from the numerical model (see shaded areas in Figure 2b). The CZCS-derived yearly composite pigment images [*Tang et al.*, 1998] also depict higher pigment in the southwestern sea area of the Hainan Island. Therefore the tidal mixing may also induce a Chl-a front near the southwestern coast of the Hainan Island. On the other hand, it is suggested that the present SeaWiFS Chl-a algorithm is in need of improvement so that the high Chl-a areas and accompanied fronts, such as in the southwestern sea area of the Hainan Island, can be indicated in the monthly averaged Chl-a distribution.

[28] As shown in Figures 2a and 3, the high Chl-a area also distributes along the coast of the Beibu Gulf so the obvious front can be seen along the Vietnam coast. However, the tidal numerical model result shows weak tidal current belt along the Vietnam coast. According to the log (h/u^3) criterion used in the present study, these weak tidal currents may be not strong enough to stir up the nutrient-rich water from the lower layer even they are located in the shallower coastal area. The possible nutrient source may be from the rivers along the coast of the Beibu Gulf (such as the Red River in the northwestern head of the gulf). Therefore the mechanism for the surface Chl-a front along the Vietnam coast is suggested not to be tidal mixing.

[29] The SST fronts have been detected in the central Beibu Gulf and in the northeastern sea area of the Hainan Island by the AVHRR-derived SST images. These fronts have obvious seasonal variations. As shown in Figure 5, the locations of these fronts are not the same as revealed by the log (h/u^3) criterion. The fronts have larger SST gradient in winter and in late autumn, small SST gradient in spring but very small SST gradient in summer. Apparently, these fronts are induced by comparable effects of the coastal SST cooling in the wintertime while the homogeneous surface warming in the summertime [*Wang et al.*, 2001]. Therefore the solar radiation and wind mixing may play an important role for the seasonal variation of these thermal fronts. In addition, these AVHRR-derived monthly mean SST images (Figure 5) do not indicate obvious front either at both ends of the Qiongzhou Strait or in the southwestern coast of the Hainan Island. It may be suggested that the tidal fronts around the Hainan Island are difficult to be detected by the monthly mean SST images. However, this deserves further studying in future.

6. Conclusions

[30] As stated above, the following conclusions can be deduced from the present study.

[31] 1. There exist fronts of the surface Chl-a concentrations in the Qiongzhou Strait, along the coasts of the Zhanjiang Peninsula and along the southwestern coast of the Hainan Island. These fronts can be considered as tidal fronts. Strong tidal currents, as revealed by the tidal numerical model, stir up the nutrient-rich water from the lower layer so as to make these areas have higher Chl-a concentrations. The clear fronts are thus formed in these areas as detected by the SeaWiFS-derived Chl-a concentrations. The locations of contour lines log (h/u^3) = 2.9 $\sim$ 3.0 are in good agreement with the frontal positions detected by the satellite observations.

[32] 2. Different tidal constituent makes different contribution for tidal mixing in the studied area. Numerical model result shows that the tidal mixing in the Qiongzhou Strait is mainly induced by the M_2, K_1, and O_1 tidal constituents while the tidal mixing in the southwestern coastal area of the Hainan Island is due to the K_1 and O_1 tidal constituents.

[33] **Acknowledgments.** This study is jointly supported by the Key Project (98-Z-179) of Fujian Province of China, by the Research and Development Applying Advanced Computational Science and Technology, Japan Science and Technology Corporation, and by the Japan Society for the Promotion of Science. The study is partly supported by "Special Coordination Funds for Promoting Science and Technology" of MEXT, Japan. The work was conducted while Hu was visiting the Ocean Variation Laboratory, Center for Atmospheric and Oceanic Studies, Tohoku University, Japan. We would like to express our great appreciations to Wataru Takahashi for his assistance in making Figure 4 and to two anonymous reviewers for their perceptive comments. Thanks are also extended to those who distributed the AVHRR, SeaWiFS, TOPEX/Poseidon and ETOPO5 data sets.

References

Belkin, I., New challenge: Ocean fronts, *J. Mar. Syst.*, *37*, 1–2, 2002.

Belkin, I., and M. Spall, New old frontier: Ocean fronts, *Dyn. Atmos. Ocean.*, *36*, 1–2, 2002.

Blumberg, A. F., and G. L. Mellor, A description of a three-dimensional coastal ocean circulation model, in *Three-Dimensional Coastal Ocean Models*, *Coastal Estuarine Stud.*, vol. 4, edited by N. Heaps, pp. 1–16, AGU, Washington, D. C., 1987.

Bowers, D. G., and J. H. Simpson, Mean position of tidal fronts in European-shelf seas, *Cont. Shelf Res.*, *7*, 35–44, 1987.

Cao, D. Z., and G. H. Fang, A numerical model for tides and tidal currents in the northern South China Sea (in Chinese with English abstract), *Trop. Oceanol.*, *9*, 63–70, 1990.

Chu, P. C., and G. H. Wang, Seasonal variability of thermohaline front in the central South China Sea, *J. Oceanogr.*, *59*, 65–78, 2003.

Fang, G. H., Tide and tidal current charts for the marginal seas adjacent to China, *Chin. J. Oceanol. Limnol.*, *4*, 1–16, 1986.

Fang, G. H., W. Z. Zheng, Z. Y. Chen, and J. Wang, *Analysis and Prediction of Tide and Tidal Current* (in Chinese), 474 pp., China Ocean, Beijing, 1986.

Fang, G. H., Y. K. Kwok, K. J. Yu, and Y. H. Zhu, Numerical simulation of principal tidal constituents in the South China Sea, Gulf of Tonkin and Gulf of Thailand, *Cont. Shelf Res.*, *19*, 845–869, 1999.

Hsueh, Y., and B. Cushman-Roisin, On the formation of surface to bottom fronts over steep topography, *J. Geophys. Res.*, *88*, 743–750, 1983.

Hu, J. Y., H. Kawamura, H. S. Hong, F. Kobashi, and Q. Xie, Tidal features in the China Seas and their adjacent areas derived from TOPEX/Poseidon altimeter data, *Chin. J. Oceanol. Limnol.*, *19*, 293–305, 2001.

Huang, Q. Z., W. Z. Wang, and J. C. Chen, Tides, tidal currents and storm surge set-up of South China Sea, in *Oceanology of China Sea 1*, edited by D. Zhou et al., pp. 113–122, Kluwer Acad., Norwell, Mass., 1994.

Li, S. H., H. Y. Xia, S. H. Liang, and R. X. Mo, Characteristics of tidal currents and residual currents in the seas adjacent to Guangxi (in Chinese with English abstract), *Mar. Sci. Bull.*, *20*, 11–19, 2001.

Lie, H. J., Tidal fronts in the southeastern Hwanghae (Yellow Sea), *Cont. Shelf Res.*, *9*, 527–546, 1989.

Liu, A. J., and Y. T. Zhang, Numerical prediction and analysis of the tide in Beibu Bay (in Chinese with English abstract), *Oceanol. Limnol. Sin.*, *28*, 640–645, 1997.

Loder, J. W., and D. A. Greenberg, Predicted positions of tidal fronts in the Gulf of Maine region, *Cont. Shelf Res.*, *6*, 397–414, 1986.

Manh, D. V., and T. Yanagi, A three-dimensional numerical model of tides and tidal currents in the Gulf of Tongking, *Mer*, *35*, 15–22, 1997.

Manh, D. V., and T. Yanagi, A study on residual flow in the Gulf of Tongking, *J. Oceanogr.*, *56*, 59–68, 2000.

Mellor, G. L., Users guide for a three-dimensional, primitive equation, numerical ocean model, pp. 1–41, Program in Atmos. and Oceanic Sci., Princeton Univ., Princeton, N. J., 1998.

Pingree, R. D., and D. K. Griffiths, Tidal fronts on the shelf seas around the British Isles, *J. Geophys. Res.*, *83*, 4615–4622, 1978.

Qi, J. H., and Y. S. Su, Numerical simulation of the tide-induced continental front in the Yellow Sea (in Chinese with English abstract), *Oceanol. Limnol. Sin.*, *29*, 247–254, 1998.

Shi, M. C., C. S. Cheng, Q. C. Xu, H. C. Lin, G. M. Liu, H. Wang, F. Wang, and J. H. Yan, The role of Qiongzhou Strait in the seasonal variation of the South China Sea circulation, *J. Phys. Oceanogr.*, *32*, 103–121, 2002.

Simpson, J. H., The shelf-sea fronts: Implications of their existence and behaviour, *Philos. Trans. R. Soc. London, Ser. A*, *302*, 531–546, 1981.

Simpson, J. H., and D. Bowers, Shelf sea fronts' adjustments revealed by satellite IR imagery, *Nature*, *280*, 648–651, 1979.

Simpson, J. H., and D. Bowers, Models of stratification and frontal movement in shelf seas, *Deep Sea Res.*, *28*, 727–738, 1981.

Simpson, J. H., and J. R. Hunter, Fronts in the Irish Sea, *Nature*, *250*, 404–406, 1974.

Simpson, J. H., D. G. Hughes, and N. C. G. Morris, Fronts on the continental shelf, *J. Geophys. Res.*, *83*, 4607–4614, 1978.

Stigebrandt, A., A note on the locus of a shelf front, *Tellus, Ser. A*, *40*, 439–442, 1988.

Sun, H. L., and W. M. Huang, Three-dimensional numerical simulation for tide and tidal current in the Beibu Gulf (in Chinese with English abstract), *Acta Oceanol. Sin.*, *23*, 1–8, 2001.

Tang, D. L., I. H. Ni, F. E. Müller-Karger, and Z. J. Liu, Analysis of annual and spatial patterns of CZCS-derived pigment concentrations on the continental shelf of China, *Cont. Shelf Res.*, *18*, 1493–1515, 1998.

Tang, D. L., H. Kawamura, M. A. Lee, and T. V. Dien, Seasonal and spatial distribution of chlorophyll-a and water conditions in the Gulf of Tonkin, South China Sea, *Remote Sens. Environ.*, *85*, 475–483, 2003.

Wang, D. X., Y. Liu, Y. Q. Qi, and P. Shi, Seasonal variability of thermal fronts in the northern South China Sea from satellite data, *Geophys. Res. Lett.*, *28*, 3963–3966, 2001.

Wang, D. X., L. Luo, Y. Liu, and S. Y. Li, Seasonal and interannual variability of thermal fronts in the Tonkin Gulf, paper presented at Third International Asia-Pacific Environmental Remote Sensing Symposium, SPIE Int. Soc. for Opt. Eng., Bellingham, Wash., 2002.

Xing, J. X., and A. M. Davies, A three-dimensional baroclinic model of the Irish Sea: Formation of thermal fronts and associated circulations, *J. Phys. Oceanogr.*, *31*, 94–114, 2001.

Yanagi, T., and T. Koike, Seasonal variation in thermohaline and tidal fronts, Seto Inland Sea, Japan, *Cont. Shelf Res.*, *7*, 149–160, 1987.

Yanagi, T., and H. Tamaru, Temporal and spatial variations in a tidal front, *Cont. Shelf Res.*, *10*, 615–627, 1990.

Yanagi, T., S. Igawa, and O. Matsuda, Tidal front at Osaka Bay, Japan, in winter, *Cont. Shelf Res.*, *15*, 1723–1735, 1995.

Yanagi, T., T. Takao, and A. Morimoto, Co-tidal and co-range charts in the South China Sea derived from satellite altimetry data, *Mer*, *35*, 85–93, 1997.

Ye, A. L., and I. S. Robinson, Tidal dynamics in the South China Sea, *Geophys. J. R. Astron. Soc.*, *72*, 691–707, 1983.

Yu, M., A preliminary study of tidal characteristics in the South China Sea (in Chinese), *Acta Oceanol. Sin.*, *6*, 293–300, 1984.

J. Y. Hu, Marine Environmental Laboratory of Ministry of Education, Institute of Subtropical Oceanography, Xiamen University, Fujian 361005, China. (hujy@xmu.edu.cn)

H. Kawamura and D. L. Tang, Center for Atmospheric and Oceanic Studies, Institute of Hydrobiology, Faculty of Science, Tohoku University, Sendai 980-8578, Japan. (kamu@ocean.caos.tohoku.ac.jp)